Thermal Behavior of a Simultaneous Charging and Discharging Concrete Bed During a Heating Cycle

Adeyanju A.A.*‡, Manohar K.**

*Mechanical Engineering Department, Ekiti State University

**Mechanical and Manufacturing Engineering Department, University of West Indies

anthonyademolaadeyanju@yahoo.co.uk, krishpersad.manohar@sta.uwi.edu

‡Corresponding Author; Adeyanju A. A., Mechanical Engineering Department, Ekiti State University, P.M.B. 5363, Ado-Ekiti, Nigeria, +2348037891575, anthonyademolaadeyanju@yahoo.co.uk

Received: 16.4.2013 Accepted: 24.5.2013

Abstract- This study developed a mathematical model from consideration of the basic phenomena of heat transfer to predict the thermal behavior of a simultaneous charging, storage and discharging system during a heating cycle. A solution to the complex mathematical model was assumed in the form of a general equation for which the constants in the equation were determined. The mathematical model simulated an air packed bed storage system coupled to a flat plate solar collector which received intermittent solar radiation and supplied it in sinusoidal form to the packed bed. Finite Fourier series analysis with the first three harmonic terms was applied to the solution of the equation. Experiments were conducted by charging the packed bed system from a flat plate solar collector of area 1.5m^2. The experimental results showed an average discharge temperature of 50.75 ^{o}C over the period of 7.00 hr to 17.00 hr compared to the theoretically predicted average value of 50.40 ^{o}C.

Keywords- Concrete, Packed-bed storage, Simultaneous, Charging and Discharging, Heating Cycle.

1. Introduction

The thermal energy storage (TES) can be defined as the temporary storage of thermal energy at high or low temperatures. The TES is not a new concept, and has been used for centuries. Energy storage can reduce the time or rate mismatch between energy supply and energy demand, and it plays an important role in energy conservation.

Energy storage improves performance of energy systems by smoothing supply and increasing reliability. For example, storage would improve the performance of a power generating plant by load leveling. The higher efficiency would lead to energy conservation and improve cost effectiveness.

Some of the renewable energy sources can only provide energy intermittently. Although the sun provides an abundant, clean and safe source of energy, the supply of this energy is periodic following yearly and diurnal cycles; it is intermittent, often unpredictable

A thermal-storage unit in which particulate materials contained in an insulated vessel is known as packed bed (pebble bed or rock pile) storage unit. It uses the heat capacity of loosely packed particulate materials to store energy. Fluid, usually air, is circulated through the bed to add or remove energy.

The most commonly used solids are rocks, concrete, clays and walls [1, 2]. The materials are invariably in porous form and heat is stored or extracted by the flow of a gas or a liquid through the pores or voids. Air systems have a number of advantages compared to those using liquid and phase transition heat transfer media. There are elimination in problem of freezing and boiling in the collectors and reduction in corrosion. Well-designed packed beds have several characteristics that are desirable for solar energy applications [9] such as:

- The heat transfer coefficient between the air and the solid is high, which promotes thermal stratification.
- The costs of storage material and container are low.
- The conductivity of the bed is low when there is no air flow.

- The pressure drop through the bed is low.

In analyzing packed bed storage, it should be recognized that both the solid and the air change temperature in the direction of air flow and generally there are temperature differentials between the solid and the air.

Consequently, it becomes necessary to write separate energy balance equations for the solid and the air with the assumption that the forced air flow is one dimensional, system properties are constant, conduction heat transfer along the bed is negligible and heat loss to the environment does not occur, the thermal behavior of the solid and the air, respectively can be described by the following two coupled partial differential equations [3].

$$A\rho_b C_b (1-\varepsilon)\, dT/dt = Ah_v (T_f - T_b) \quad (1)$$

$$A\rho_f C_f \varepsilon = -mC_f dT - Ah_v (T_f - T_b) \quad (2)$$

The performance of packed-bed thermal storage unit is a function of the physical and thermal characteristics of the particles [3]. The physical parameters include average particle diameter; the void fraction (ε); the surface area shape factor (α). The thermal properties are the specific heat, thermal diffusivity, thermal resistivity, thermal conductivity and thermal coefficient of expansion.

Besides high thermal durability, the storage concrete has to fulfill numerous requirements [4]. A high heat capacity and thermal conductivity will reduce the costs of the heat exchanger and thermal insulation. Furthermore the concrete itself has to be economical and easily workable.

This study developed a mathematical model to determine the thermal performance of the packed bed storage system which utilized spherical shaped concrete imbedded with copper tube as the storage medium.

Thermal storage in concrete relies on sensible heat storage where the stored thermal energy is defined by the heat capacity of the concrete and the temperature difference between the charged and the discharged states.

Mathematical expressions for the temperature distribution in the solid and in the fluid have been derived as a function of time and packed bed height. Schumann's model was performed on each of the fluid and solid phases yielding two coupled partial differential equations, two phase linear models. The two energy balance equations which explained the transfer of heat were:

For Fluid Phase:

$$\frac{A\rho_f C_f \varepsilon\, \partial T_f}{\partial t} = \frac{-M_f C_f \partial T_f}{\partial x} + h_v A (T_s - T_f) \quad (3)$$

For Solid Phase:

$$\frac{A\rho_S C_S (1-\varepsilon)\, \partial T_s}{\partial t} = h_v A (T_f - T_s) \quad (4)$$

In Schumann's two phase model, several assumptions were made. The transfer of heat by conduction in the fluid itself or in the solid itself was small and was neglected. In addition, the thermal losses to the environment were zero, adiabatic prism. The thermal constants were independent of the temperature.

The transient response of a solid sensible heat storage system which was composed of a number of rectangular cross-sectional channels for the flowing fluid, connected in parallel and separated by the heat storage material was studied by Schmidt and Szego [8]. The equations which govern the transient response of the storage unit are the one dimensional conservation of energy equations for the moving fluid and the two dimensional transient heat conduction equations for the storage material.

The governing differential equations were:

For moving fluid:

$$\rho_f C_f A \left\{ \frac{\partial T_f}{\partial t} - \frac{v\, \partial T_f}{\partial x} \right\} = hP (T_W - T_f) \quad (5)$$

For storage material:

$$\left(\frac{1}{\alpha}\right)\left(\frac{\partial T_s}{\partial t}\right) = \left[\frac{\partial^2 T_s}{\partial x^2} + \frac{\partial^2 T_s}{\partial y^2}\right] \quad (6)$$

These two equations were solved by using finite difference techniques. A set of curves were presented to describe the dimensionless parameters which characterized the transient behavior.

Riaz presented a simple one dimensional single phase conductivity model for transient analysis of a packed bed which accounts for the fluid convective motion, the air-rock heat transfer, axial bed conduction, and internal particle conduction in which air and rock are at the same temperature [7]. The model was:

$$\frac{\partial T}{\partial t} + \frac{V \partial T}{\partial x} = \frac{\alpha_s \partial^2 T_s}{\partial x^2} \quad (7)$$

Where,

$$V = \frac{V_a \rho_a C_a}{\rho_s C_s} \quad (8)$$

And

$$\alpha_s = \frac{\text{ks}}{\rho_s C_s} \quad (9)$$

From this equation, if the conduction term is zero $(\alpha = 0)$, the equation is reduced to the convection motion of thermal wave traveling at the reduced velocity V.

By comparing this model with the two phase Schumann model, Riaz noted that the results for both models almost coincide for sufficiently large values of dimensionless time $(t > 10); \frac{1}{2}$ for small (t), the agreement is within 10%. He recommended, for the step response of time varying inlet temperature, that the combined effects of axial conductivity and air rock heat transfer be incorporated in both models.

The equivalent relationships were:

For Schumann's model:

$$\frac{1}{h_{eq}} = \frac{i}{h_v} + \frac{k_s}{(v_a \rho_a C_a)^2} \quad (10)$$

For single phase model:

$$k_{eq} = k_s + \frac{(v_a \rho_a C_a)^2}{h_v} \quad (11)$$

He concluded that the characteristics of the step response are presented in the form of generalized plots portraying the time space profile of the thermal waves. These curves represent so called thermoclines used for preliminary design purposes and for estimating the dynamic performance of packed storage systems.

2. Methodology

2.1. Test Procedures

Fig. 1 shows the schematic of flat plate solar collector experiment. A forward curved blade centrifugal fan driven by a 373 W electric motor was employed to deliver air through the solar collector. Inlet air temperature at the entrance of the collector was controlled by thermostat.

Three runs of air flow rates were conducted for the 0.065m, 0.08 and 0.11m diameter spherical shaped concrete at the normal drop. The designed air flow rates were 0.0094m^3/s, 0.013m^3/s, and 0.019m^3/s per square meter of total cross sectional area of the storage tank. The corresponding superficial velocities were approximately 0.1m/s, 0.15m/s and 0.20m/s.

As soon as the air enters the storage tank into the packed bed, temperature measurements of air, ambient temperature, absorber plate temperature, collector air temperature at the inlet and outlet, concrete surfaces, copper tube surfaces, concrete core and inside of the copper tube were recorded at four levels via a data logger connected with the computer. These four levels were located at different heights above the base, 117.5cm, 235cm, 352.5cm, and 470cm.

Temperatures were measured at the storage tank inlet and outlet and copper tube inlet and outlet through the copper-constantan thermocouples via a data logger connected to a computer. The measurements were taken automatically at an interval of 10 minutes for between 10 to 12 hours.

Type J thermocouples were used for all tests performed. This Pico instrument was capable of 0.1^{o}C resolution with readings displayed in ^{o}C and capable of continuously recording and exporting data to a remote computer.

The copper tube was of type L and of 0.00635m standard size. The outside diameter of the copper tube was 0.02223m, the inside diameter was 0.01994m, wall thickness of 0.01143m, length 1.32m, number of copper tubes was 4 of two passes with radius 0.115m. The spherical shaped concrete was made of ratio 1:1.2:1.1 of cement, sand and gravel, respectively.

The entry and exit lengths were 0.65 and 0.96m respectively, including the inlet plenum and outlet plenum height of 0.3 m each.

In order to test the storage capacity of the spherical shaped concrete and the copper tube, the measurements were also taken during the night period when the simulated heat was no longer in supply to the packed bed.

Upon analysis of all measuring equipment, the error calculated for these experiments was found to be ±5%.

The air velocity profile in the duct was measured by a pitot-static tube. The air flow rate was the product of the average velocity and the duct cross-sectional area. Wind velocity above the solar collector was measured by a cup anemometer. Readings were done instantaneously.

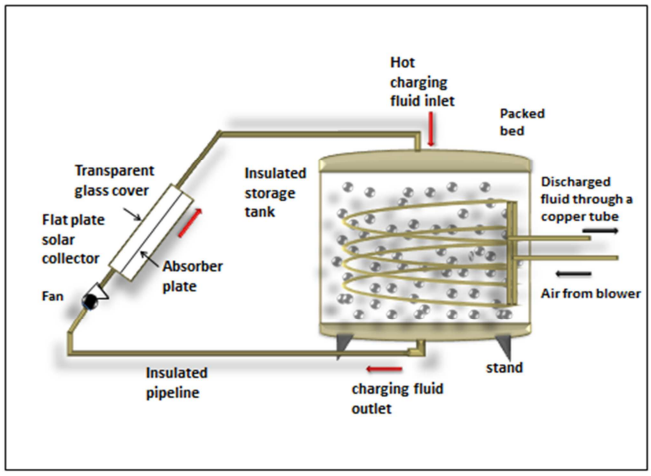

Fig. 1. Schematic of Flat Plate Solar Collector Experiment

2.2. Modeling of Air Temperature Distribution in the Bed

To predict the temperature distribution of air passing through the packed bed (spherical shaped concrete embedded with copper tube), mathematical expression from the fundamentals of heat and mass transfer was utilized.

The following assumptions were made:

- Physical and thermal properties of the fluid and solid material in the packed bed are constant
- Uniform heat transfer coefficient
- Mean velocity of the fluid in the packed bed is constant
- Radial heat transfer for air and concrete were neglected
- No chemical reaction
- No mass transfer
- Thermal gradients within the solid particles were neglected

Consider a packed bed with a cross-sectional area (A) and length (L). The plane of the cross-section was divided into the area of fluid (A_f) and area of the spherical concrete

together with area of copper tube ($A_{c,ct}$) since the void fraction affects the heat capacity of the packed bed.

Voids fraction is defined as the ratio of area of the fluid (A_f) to the total area of fluid plus area of the spherical concrete and copper tube ($A_{f+}A_{c,\,ct}$) at the cross-section of the packed bed as follows:

$$\text{Void fraction or porosity } \varepsilon = \frac{\left(A_f\right)}{\left(A_f + A_{c,ct}\right)} \tag{12}$$

In this analysis, an element with length ΔX was considered as indicated in Fig. 2. A_{sur} is the surface area through which heat passes per unit length of the packed bed storage section (m^2/m).

The fluid superficial velocity through the bed $\left(V_{sl}\right)$ can be determined by the following equation since it takes the fluid a time, Δt to move through a differential segment of the packed bed ΔX.

$$V_{sl} = \frac{v_f}{A_f} = \frac{\Delta X}{\Delta t} \tag{13}$$

$where, v_f$ = Airflow per unit time

Three fundamental equations can be written as follows to explain heat exchange between the air and packed materials in the elemental volume ($A_{f+}A_{c,\,ct}$) ΔX in order to get the inlet air temperature distribution.

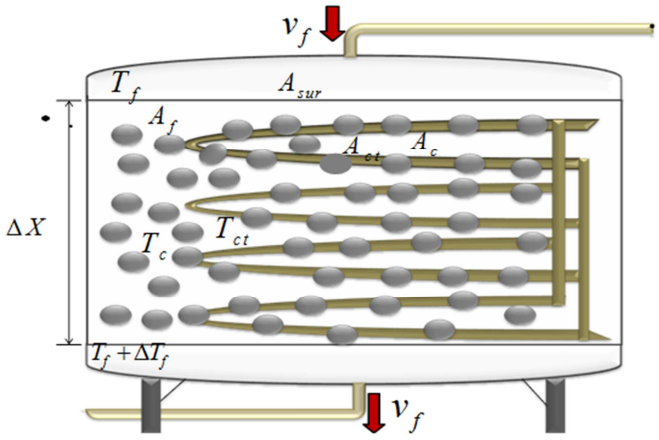

Fig. 2. Schematic showing the segment of the mathematical model of the packed bed

Also, another fundamental equation was derived for the temperature of air flowing inside the copper tube.

- The energy equation of air moving a distance ΔX through the elemental part of the bed with inlet air temperature (T_f) and an outlet fluid temperature ($T_{f\,+}\Delta T_f$) was presented using the following equations from the first law of thermodynamics for a closed system:

$$Q = w + \Delta u \tag{14}$$

$where, Q$ = Heat transfer rate

w = Work transfer rate

Δu = The rate of change of internal thermal energy with time

Since $w = 0$,

$$\therefore Q_f = \Delta u \tag{15}$$

$$but, \Delta u = m_f C_f dT \tag{16}$$

$$and, m_f = \rho_f v_f \tag{17}$$

$$\therefore \Delta u = \rho v_f C_f dT \tag{18}$$

$$\therefore Q_f = v_f \rho_f C_f \Delta T_f \tag{19}$$

$where, Q_f$ = Heat gain by the fluid *(KJ/s)*

ρ_f = The average density of air entering the bed *(Kg/m^3)*

C_f = The specific heat capacity of air entering the bed *(KJ/KgK)*

(i) The energy gain or loss to or from the spherical concrete materials and the copper tube which is proportional to their volume, the physical and thermal properties of the concrete and copper tube, and the change in the concrete and copper tube temperature over time interval Δt. The energy equation for this case can be written as:

$$Q_c = -A_c \Delta X \rho_c C_c \frac{\Delta T_c}{\Delta t}$$

also,

(20)

$$Q_{ct} = -A_{ct} \Delta X \rho_{ct} C_{ct} \frac{\Delta T_{ct}}{\Delta t}$$

(21)

- The exchange of heat between the air and the packed materials at the interface area was taken to be proportional to the surface area, *(A_{sur})* and also, to be proportional to the temperature difference. The energy transfer equation for this case can be written as:

$$Q = UA_{sur} \Delta X \left(T_c - T_f\right) \tag{22}$$

$$Q = UA_{sur} \Delta X \left(T_{ct} - T_f\right) \tag{23}$$

The convective heat transfer coefficient may be obtained by applying the following formula:

$$U = \frac{h_v \left(A_f + A_{c,ct}\right)}{A_{sur}} \tag{24}$$

Given the stated assumptions, these three energy equations described the exchange of heat between the heated air and packed materials.

$$Q_f = Q_c = Q_{ct} = Q \tag{25}$$

These quantities may be eliminated between these three major equations giving the following two equations:

(i) For the fluid:

$$v_f \rho_f C_f \Delta T_f = UA_{sur} \Delta X \left(T_c - T_f \right) \tag{26}$$

$$v_f \rho_f C_f \Delta T_f = UA_{sur} \Delta X \left(T_{ct} - T_f \right) \tag{27}$$

Rearranging equations 26 and 27 gives:

$$\frac{v_f \rho_f C_f \Delta T_f}{\Delta X} = UA_{sur} T_c - UA_{sur} T_f \tag{28}$$

$$\frac{v_f \rho_f C_f \Delta T_f}{\Delta X} = UA_{sur} T_{ct} - UA_{sur} T_f \tag{29}$$

As ΔX tends to zero, a first partial differential equation evolved and can be written as:

$$v_f \rho_f C_f \frac{\partial T_f}{\partial X} + UA_{sur} T_f = UA_{sur} T_c \tag{30}$$

$$v_f \rho_f C_f \frac{\partial T_f}{\partial X} + UA_{sur} T_f = UA_{sur} T_{ct} \tag{31}$$

(ii) For the spherical concrete material:

$$\frac{-A_c \Delta X \rho_c C_c \Delta T_c}{\Delta t} = UA_{sur} \Delta X \left(T_c - T_f \right) \tag{32}$$

As $\Delta t \to 0$, the second partial differential equation is derived and can be written as:

$$-A_c \rho_c C_c \frac{\partial T_c}{\partial t} + UA_{sur} T_f = UA_{sur} T_c \tag{33}$$

(iii) For the copper tube:

$$\frac{-A_c \Delta X \rho_c C_c \Delta T_c}{\Delta t} = UA_{sur} \Delta X \left(T_{ct} - T_f \right) \tag{34}$$

As $\Delta t \to 0$, the third partial differential equation is derived and can be written as:

$$-A_c \rho_c C_c \frac{\partial T_c}{\partial t} + UA_{sur} T_f = UA_{sur} T_{ct} \tag{35}$$

The next thing in this analysis was the elimination of T_c and T_{ct}:

Differentiate equation (30) and (31) with respect to time to give:

$$v_f \rho_f C_f \frac{\partial^2 T_f}{\partial X \partial t} + UA_{sur} \frac{\partial T_f}{\partial t} = UA_{sur} \frac{\partial T_c}{\partial t} \tag{36}$$

$$v_f \rho_f C_f \frac{\partial^2 T_f}{\partial X \partial t} + UA_{sur} \frac{\partial T_f}{\partial t} = UA_{sur} \frac{\partial T_{ct}}{\partial t} \tag{37}$$

Multiplying equation (36) and (37) by $\frac{A_c \rho_c C_c}{UA_{sur}}$ and $\frac{A_{ct} \rho_{ct} C_{ct}}{UA_{sur}}$, respectively, lead to the following equations:

$$\left(\frac{A_c \rho_c C_c}{UA_{sur}} \right) \left(v_f \rho_f C_f \frac{\partial^2 T_f}{\partial X \partial t} \right) + \left(A_c \rho_c C_c \right) \frac{\partial T_f}{\partial t} = \left(A_c \rho_c C_c \right) \frac{\partial T_c}{\partial t} \tag{38}$$

$$\left(\frac{A_c \rho_c C_c}{UA_{sur}} \right) \left(v_f \rho_f C_f \frac{\partial^2 T_f}{\partial X \partial t} \right) + \left(A_c \rho_c C_c \right) \frac{\partial T_f}{\partial t} = \left(A_c \rho_c C_c \right) \frac{\partial T_c}{\partial t} \tag{39}$$

Combine equation (30), (36), (38) and (31), (37), (39), and then eliminate the temperature T_c and $T_{ct,}$ respectively:

$$\begin{aligned} &v_f \rho_f C_f \frac{\partial T_f}{\partial X} + UA_{sur} T_f - UA_{sur} + A_c \rho_c C_c \frac{\partial T_c}{\partial t} - UA_{sur} T_f + UA_{sur} T_c + \\ &\left(\frac{A_c \rho_c C_c}{UA_{sur}} \right) \left(v_f \rho_f C_f \frac{\partial^2 T_f}{\partial X \partial t} \right) + \left(A_c \rho_c C_c \right) \frac{\partial T_f}{\partial t} - \left(A_c \rho_c C_c \right) \frac{\partial T_c}{\partial t} = 0 \end{aligned} \tag{40}$$

$$\begin{aligned} &v_f \rho_f C_f \frac{\partial T_f}{\partial X} + UA_{sur} T_f - UA_{sur} + A_a \rho_a C_a \frac{\partial T_a}{\partial t} - UA_{sur} T_f + UA_{sur} T_a + \\ &\left(\frac{A_a \rho_a C_a}{UA_{sur}} \right) \left(v_f \rho_f C_f \frac{\partial^2 T_f}{\partial X \partial t} \right) + \left(A_a \rho_a C_a \right) \frac{\partial T_f}{\partial t} - \left(A_a \rho_a C_a \right) \frac{\partial T_a}{\partial t} = 0 \end{aligned} \tag{41}$$

$$\therefore v_f \rho_f C_f \frac{\partial T_f}{\partial X} + \left(\frac{A_c \rho_c C_c}{UA_{sur}} \right) \left(v_f \rho_f C_f \frac{\partial^2 T_f}{\partial X \partial t} \right) + \left(A_c \rho_c C_c \right) \frac{\partial T_f}{\partial t} = 0 \tag{42}$$

dso,

$$v_f \rho_f C_f \frac{\partial T_f}{\partial X} + \left(\frac{A_a \rho_a C_a}{UA_{sur}} \right) \left(v_f \rho_f C_f \frac{\partial^2 T_f}{\partial X \partial t} \right) + \left(A_a \rho_a C_a \right) \frac{\partial T_f}{\partial t} = 0 \tag{43}$$

Combining equation (42) and (43) produced:

$$\begin{aligned} &v_f \rho_f C_f \frac{\partial T_f}{\partial X} + \left(\frac{\left(A_c \rho_c C_c \right) \left(A_a \rho_a C_a \right)}{UA_{sur}} \right) \left(v_f \rho_f C_f \frac{\partial^2 T_f}{\partial X \partial t} \right) + \\ &\left(A_c \rho_c C_c \right) \left(A_a \rho_a C_a \right) \frac{\partial T_f}{\partial t} = 0 \end{aligned} \tag{44}$$

$$\begin{aligned} &v_f \rho_f C_f \left(\frac{\partial T_f}{\partial X} \right) + \left\{ \left(\frac{\left(A_c \rho_c C_c \right) \left(A_a \rho_a C_a \right) \left(v_f \rho_f C_f \right)}{UA_{sur}} \right) \left(\frac{\partial^2 T_f}{\partial X \partial t} \right) \right\} + \\ &\left(A_c \rho_c C_c \right) \left(A_a \rho_a C_a \right) \frac{\partial T_f}{\partial t} = 0 \end{aligned} \tag{45}$$

$$\begin{aligned} &but, A_{sur} = \left(\frac{\pi d_c^2}{1/6 \pi d_c^3} \right) \left(\frac{2 \pi r_{ct} h_{ct}}{\pi r_{ct}^2 h_{ct}} \right) \left(1 - \varepsilon \right) A_{st} L \\ &A_{sur} = \frac{24 A_{st} \left(1 - \varepsilon \right) L}{d_c d_{ct}} \end{aligned} \tag{46}$$

A_{sur} can be determined in terms of average particle diameter d_c, d_{ct} for the differential control volume since the concrete pellets are spheres of uniform size and cylindrical copper tube.

$$v_f\rho_f C_f\left(\frac{\partial T_f}{\partial X}\right)+\left\{\left(\frac{(A_c\rho_c C_c)(A_a\rho_a C_a)(v_f\rho_f C_f)}{U\left[\frac{24A_s(1-\varepsilon)L}{d_c d_a}\right]}\right)\left(\frac{\partial^2 T_f}{\partial X\partial t}\right)\right\}+ (A_c\rho_c C_c)(A_a\rho_a C_a)\frac{\partial T_f}{\partial t}=0 \quad (47)$$

$$v_f\rho_f C_f\left(\frac{\partial T_f}{\partial X}\right)+\left\{\left(\frac{(A_c\rho_c C_c)(A_a\rho_a C_a)(v_f\rho_f C_f)d_c d_a}{24UA_s(1-\varepsilon)L}\right)\left(\frac{\partial^2 T_f}{\partial X\partial t}\right)\right\}+ (A_c\rho_c C_c)(A_a\rho_a C_a)\frac{\partial T_f}{\partial t}=0 \quad (48)$$

Equation (48) is a partial differential equation for the fluid temperature (T_f) within the packed bed and can be evaluated at any position and time at different stage of the packed bed.

This equation was derived and solved analytically for a step input function by Schuman [8]. His solutions were presented as a series of sinusoidal curve.

If equation (48) is a realistic representation of the air temperature in a packed bed and the assumptions listed previously are valid, then various solutions to this equation can be considered. In general, prediction of the outlet air temperature from the bed would have to be approached by some form of numerical solution.

The outlet temperature from the solar collector which is sinusoidal in nature due to intermittent nature of the solar radiation may be treated as a periodic function with a periodic time of twenty four hours and mathematically a periodic function can often be represented by the sum of a series cosine and sine terms (Fourier series).

It is therefore of some interest to examine the solution of equation (48) when the input temperature varies sinusoidally for many consecutive periods. In other words, to ignore the transient response and concentrate on the periodic response to a sinusoidal forcing function. Equation (48) can thus be rewritten as:

$$Z_C\left(\frac{\partial T_f}{\partial X}\right)+Z_D\left(\frac{\partial^2 T_f}{\partial X\partial t}\right)+Z_E\frac{\partial T_f}{\partial t}=0 \quad (49)$$

Where,

$$Z_C = v_f\rho_f C_f \quad (50a)$$

$$Z_D=\frac{(A_c\rho_c C_c)(A_a\rho_a C_a)(v_f\rho_f C_f)d_c d_a}{24UA_s(1-\varepsilon)L} \quad (50b)$$

$$Z_E=(A_c\rho_c C_c)(A_{ct}\rho_{ct}C_{ct}) \quad (50c)$$

Mathematically, this condition may be presented as the following formula since the input temperature varies sinusoidally:

$$T_f = T_{amp}\sin\omega t \quad (51)$$

The temperature of the air at any point in the bed at any time after transients have died away might be presented rearranging equation (51) as:

$$T_f(x,t) = T_{amp}e^{-AX}\sin(\omega t - BX) \quad (52)$$

Where, T_f = the fluid temperature at any distance X and any time t

T_{amp} = amplitude of the sinusoidal temperature function

X = positions in the bed

ω = angular velocity of sinusoidal temperature variation imposed on input temperature to the bed

t = time (hr)

B = phase lag (rad/l)

A = exponential decay constant per unit length

The constants A and B may be found by substituting equation (52) into equation (49).

$$\frac{\partial T_f}{\partial X}=-T_{amp}Ae^{-AX}\sin(\omega t-BX)-T_{amp}Be^{-AX}\cos(\omega t-BX) \quad (53)$$

$$\frac{\partial^2 T_f}{\partial X\partial t}=-T_{amp}Ae^{-AX}\omega\cos(\omega t-BX)-T_{amp}Be^{-AX}(-\omega)\sin(\omega t-BX) \quad (54)$$

$$\frac{\partial T_f}{\partial t} = T_{amp}e^{-AX}\omega\cos(\omega t - BX) \quad (55)$$

$$-Z_C A\sin(\omega t-BX)-Z_C B\cos(\omega t-BX)-Z_D A\omega C\cos(\omega t-BX)+ Z_D B\omega\sin(\omega t-BX)+Z_E\cos(\omega t-BX)=0 \quad (56)$$

For equation (47) to be an identity for all x and t, since sin (ωt-Bx) and cos (ωt-Bx) is not equal to zero, then the coefficients of sine and cosine must be zero.

$$-Z_C A + B\omega Z_D = 0 \quad (57)$$

$$-Z_C B + \omega Z_E - AZ_D\omega = 0 \quad (58)$$

Solving equations (57) and (58) resulted to the two constants A and B as follows:

$$A=\frac{\omega^2 Z_D Z_E}{\omega^2 Z_D{}^2 + Z_C{}^2} \quad (59)$$

$$B=\frac{\omega Z_C Z_E}{\omega^2 Z_D{}^2 + Z_C{}^2} \quad (60)$$

The values of constant A and B show that the assumed form of solution for equation (49) is valid when the forcing function is sinusoidal. Comparison can therefore be made by comparing the model equation (52) with the solar collector experimental results.

3. Application of Finite Fourier series and Measurements of Input-Output Air Temperature Passing through the Bed

To obtain a solution to a particular boundary value problem, it is necessary to expand the function into a trigonometric series. As the outlet temperature from a flat plate solar collector changes periodically as a function of time, the Fourier expansion corresponding to this function could be applied. The Fourier series may be defined as [5]:

$$F_o(t) = \frac{A_o}{2} + \sum_{k=1}^{k=n-1}\left(A_k \cos k\omega t + B_k \sin k\omega t\right) + \frac{A_n}{2}\cos \omega n t \qquad (61)$$

A_K and B_k,, the coefficients of cosine and sine terms are defined as Fourier series coefficients which can be obtained as follows:

$$A_k = \frac{1}{n} + \sum_{P=0}^{P=2n-1} F(t_p)\cos k\omega t_p \qquad k = 0, 1\ldots n \qquad (62)$$

$$B_k = \frac{1}{n} + \sum_{P=0}^{P=2n-1} F(t_p)\sin\{k\omega t_p\} \qquad k = 1, 2\ldots n\text{-}1 \qquad (63)$$

The function $F(t)$ is often given at $2n\text{-}1$ points, but it is still for $2n$ intervals. It is assumed that $F(o) = F(p)$ and P is the period of the oscillation.

Applying Fourier expansion procedure, an experiment was run using a flat plate solar collector to follow the exact profile of the discharge air temperature from an air-type solar collector model.

4. Results and Discussion

Comparison of flat plate solar collector experimental values and values obtained from the Fourier series for inlet temperature to the packed bed storage system from 7.00 hr to 17.00 hr are shown in Fig. 3 and that the predicted values increases up to the peak of 77.86°C around 15.00 hr while the solar collector experimental values increases up to 73.93 °C around the same time. Both predicted and the experimental values decreased after 15.00 hr.

It was discovered that the values for the solar collector experiment were approximately 95% close to the predicted value from the Fourier series and that the curve produces were sinusoidal in nature, this results indicates that the radiation received from the sun by the flat plate solar collector was intermittent and diffused in nature as predicted by the theoretical analysis.

The comparison of mathematical model and experimental values for discharged temperature through the copper tube at airflow rate of 0.0094, 0.013 and 0.019 m^3/s for spherical shaped concrete of size 0.065m, 0.08m and 0.11m (diameter) are shown in Fig. 4, 5 and 6, respectively.

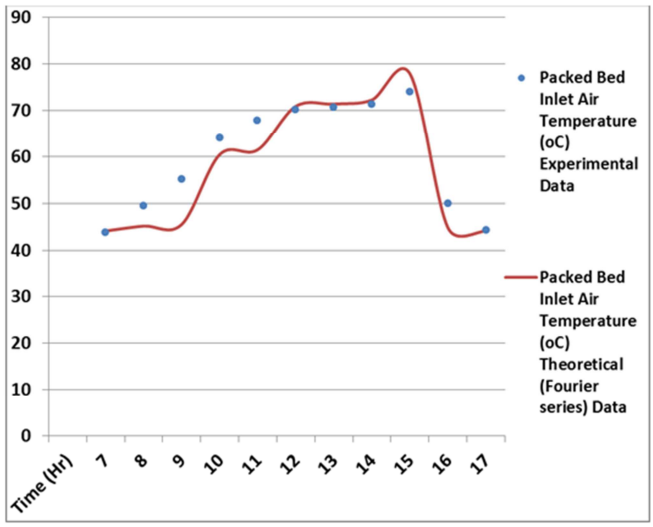

Fig. 3. Comparison of Inlet Air Temperature of Packed bed applying Fourier Series Technique with the Solar Collector Experimental Data

The comparisons were made for the period of 7.00 hr to 17.00 hr.

Spherical shaped concrete of diameter 0.11m which exhibited the highest thermal energy storage efficiency of 60.5% at 0.013m^3/s air flow rate also produced the highest and usable discharged temperature from the copper tube as shown in Fig. 5.

The measured discharged temperature result from the flat plate solar collector for spherical shaped concrete of diameter 0.11m during the period 7.00 hr., 8.00 hr.,

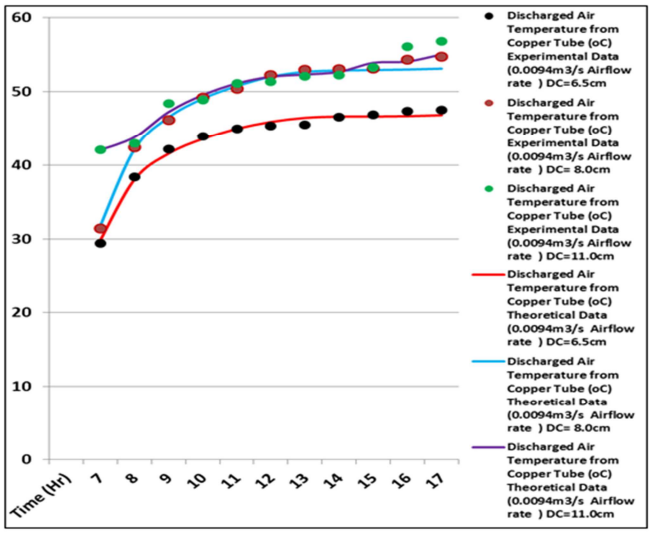

Fig. 4. Comparison of the Theoretical Discharged Air Temperature from the Copper Tube with the Solar Collector Experimental Data at 0.0094m^3/s Airflow rate

9.00 hr., 10.00 hr., 11.00 hr., 12.00 hr., 13.00 hr., 14.00 hr., 15.00 hr., 16.00 hr. and 17.00 hr. were 38.47°C, 42.85°C, 46.08 °C, 49.98 °C, 51.24 °C, 52.65 °C, 54.40 °C, 55.79 °C, 54.07 °C, 56.12 °C, and 56.97 °C, respectively, while the predicted discharged temperature from the mathematical model result for spherical shaped concrete of diameter 0.11m during the period 7.00 hr, 8.00 hr., 9.00 hr., 10.00 hr., 11.00

hr., 12.00 hr., 13.00 hr., 14.00 hr., 15.00 hr., 16.00 hr. and 17.00 hr. were 38.49°C,43.20°C, 47.18 °C, 49.78 °C, 51.41 °C, 52.86 °C, 54.12 °C, 55.03 °C, 54.60 °C, 54.18 °C, and 53.64 °C, respectively.

Taking the average of these values over the period of 7.00 hr to 17.00 hr which was 50.75 °C for the solar collector experiment and 50.40 °C for the mathematical model, good agreement within 1% between the measured values of temperature gradient in the packed bed and the predicted values obtained by the mathematical model was seen. This indicated that the experimental results do validates the predicted results.

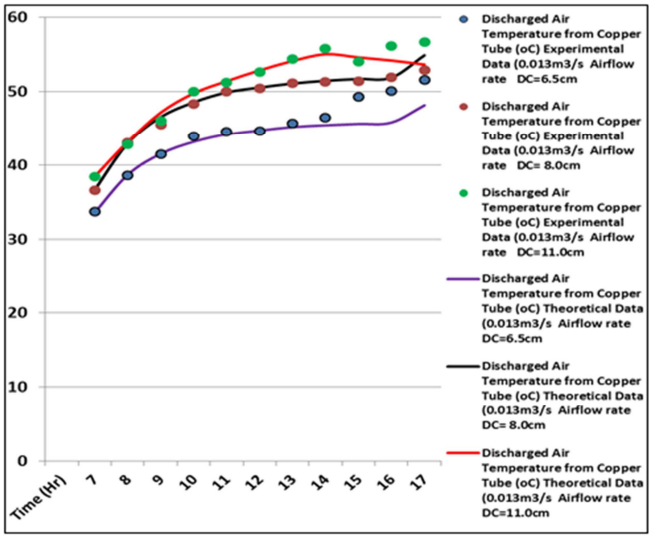

Fig. 5. Comparison of the Theoretical Discharged Air Temperature from the Copper Tube with the Solar Collector Experimental Data at 0.013m^3/s Airflow rate

The discharged temperature increased for both the experimental and the predicted results as diameter of the concrete in the packed bed increased for the tested airflow rates of 0.0094, 0.013 and 0.019 m^3/s.

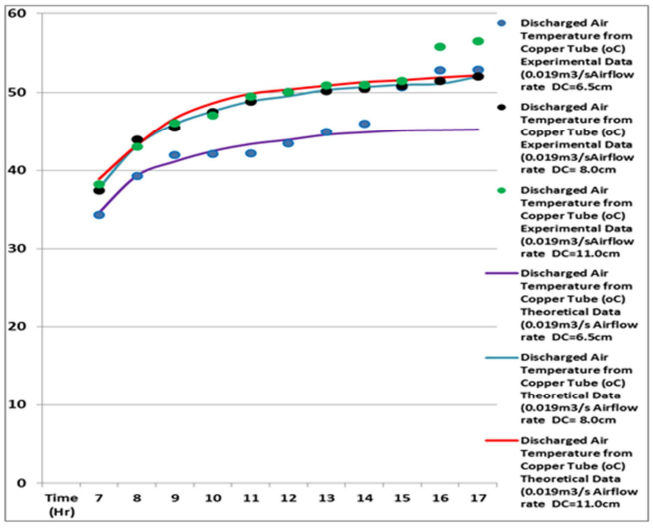

Fig. 6. Comparison of the Theoretical Discharged Air Temperature from the Copper Tube with the Solar Collector Experimental Data at 0.0194m^3/s Airflow rate

5. Conclusion

The mathematical model and experimental data was compared and the mathematical model accurately predicted the temperature within the packed bed. Good agreement within 1% between the measured values of temperature gradient in the packed bed and the predicted values was obtained by the mathematical model. The study led to the following findings and conclusions:

1. The mathematical model developed can accurately predict the temperature within the packed bed.
2. The closed form solution of the temperature variation at the steady periodic temperature trend in a packed bed can be approximated by: $F(X,t) = Te^{-AX} \sin(\omega t - BX)$
3. Good agreement has been conducted between the measured values of temperature gradient in a packed bed and the predicted values obtained by the mathematical model.
4. The values of exponential decay coefficient, A and lag coefficient, B, equations are valid for applying in the assumed form of solutions:
5. $$A = \frac{\omega^2 Z_D Z_E}{\omega^2 Z_D{}^2 + Z_C{}^2}$$

   $$B = \frac{\omega Z_C Z_E}{\omega^2 Z_D{}^2 + Z_C{}^2}$$
6. The steady intermittent input temperature variation actually led to continuous discharge temperature at the copper tube outlet.
7. A Fourier series technique of temperature discharge from a typical air type flat plate solar collector can typically be truncated at the third harmonic terms. The improvement after three harmonics was insignificant since Fourier coefficients of sine and cosine terms were very small.
8. Simulation analysis using the mathematical model may be used in the design of an air type flat plate solar collector to evaluate the collector size.

Nomenclature

A	Cross sectional area of the packed bed (m^2)
A_{sur}	The interface area between fluid and the packed materials per unit bed length *(m^2/m)*
T_b	Temperature of the bed material (K)
T_f	Temperature of the fluid material (K)
ρ_b	Density of the bed material (kg/m^3)
ρ_f	Density of the fluid (kg/m^3)
C_b	Specific heat of the bed material (J/kgK)

C_f Specific heat of the fluid (J/kgK)

t Time (s)\

x Position along bed in the flow direction (m)

m Mass flow rate of fluid (kg/s)

ε Void fraction of the bed, dimensionless (void volume/total volume of bed)

h_v is the volumetric heat transfer coefficient (W/m^3K)

G is the fluid mass velocity in kg/sm^2 of bed frontal and

d is the rock diameter (m)

Q_c Heat loss by the spherical concrete materials *(J/s)*

ρ_c The average density of the spherical concrete materials *(Kg/m^3)*

C_c The specific heat capacity of the spherical concrete materials *(J/KgK)*

Q_{ct} Heat loss by the copper tube *(J/s)*

ρ_{ct} The average density of the copper tube *(Kg/m^3)*

C_{ct} The specific heat capacity of the copper tube *(J/KgK)*

Q The rate of heat transfer *(J/s)*

U The convective heat transfer coefficients *(J/sm^2K)*

T_c The concrete temperature *(K)*

T_{ct} The copper tube temperature *(K)*

References

[1] Ataer, O.E. (2006). Storage of Thermal Energy. Encyclopedia of Life Support Systems (EOLSS) UNESCO. Oxford: EOLSS Publishers.

[2] Adeyanju, A. A (2009a). Effect of Fluid Flow on Pressure Drop in a Porous Medium of a Packed Bed. Journal of Engineering and Applied Sciences 4 (1): 83-86.

[3] Duffie, J. A., and W. A. Beckman. (2006). Solar Engineering of Thermal Processes. New York: John Wiley.

[4] Laing, D; W. D. Steinmann; R. Tamme and C. Richter. (2006). Solid Media Thermal Storage for Parabolic Trough Power Plants. Journal of Solar Energy 80 (10): 1283-1289.

[5] Mark's Standard Handbook for Mechanical Engineers. (1978). 8th Edition. New York: McGraw-Hill Book Company.

[6] Riaz, M. (1977) Analytical Solution for Single and Two Phase Models of Packed Bed Thermal Storage Systems. Journal of Heat Transfer. 99; Pp. 489-492.

[7] Schmidt, F. W. And Szego J. (1976) Transient Response of Solid Sensible Heat Thermal Storage Units Single Fluid. Transactions of the Association of Mechanical Engineers. Journal of Heat Transfer. 98. No 3. Pp.471-477.

[8] Schumann, T. E. W. (1929). Heat Transfer: A Liquid Flowing Through a Porous Prism. Journal of Heat Transfer 5: 208-212.

[9] Tiwari, G.N. 1994. Experimental Simulation of a Grain Drying System. Energy Conversion and Management Journal 1:5.